Experimental and Numerical Study of Cavitation Phenomenon in a Semi-open Impeller Centrifugal Pump

Mina L. Kerellous*
Training Sector, Mechanical Engineering Dept.
Hydro Power Plants Generation Company
Aswan, Egypt
minalttr@gmail.com

Tarek A. Mekhail
Mechanical Power Engineering Dept.
Faculty of Energy Engineering, Aswan University
Aswan, Egypt
tmalak@aswu.edu.eg

Waleed A. Abdel-Fadeel
Mechanical Power Engineering Dept.
Faculty of Energy Engineering, Aswan University
Aswan, Egypt
wfadeel@aswu.edu.eg

Hesham S. Abdel-Mohsen
Mechanical Power Engineering Dept.
Faculty of Energy Engineering, Aswan University
Aswan, Egypt
h_sayed80@energy.aswu.edu.eg

***Abstract*—In the current work, flow visualization and numerical simulation by ANSYS-FLUENT of a centrifugal pump with a semi-open impeller are utilized to verify that decreasing the speed will decrease the formation of air bubbles and hence cavitation occurrence possibilities. The purpose of the current work is to utilize two different test rigs, pumping systems, to verify that each pumping system nearly has the same reduction percentages in cavitation occurrence for the same reduction percentages of speed. This study compares two centrifugal pumps with different capacities, whereas the first pump is 0.5 hp and the second is 2 hp. They pump water using two different pumping systems with two different percentages of speed reduction for the two pumps. The results indicated that the suction pressure, which represented an indication of the cavitation status, increased due to the percentages of speed reductions of 6% and 12% (related to full pump speed) for the first pump by 8% and 21% and for the second pump by 8% and 19%, respectively.**

Computational Fluid Dynamics (CFD) numerical simulation and experimental investigations are performed on three different speeds of two laboratory centrifugal pumps with a Plexiglas casing. Numerical simulation findings show that there is an acceptable agreement with the experimental work, with an error percentage of 8.5% for the best case, and it was insured that the speed reduction by the above percentages is an active procedure to reduce the harmful effect of cavitation.

***Keywords*—Centrifugal pump cavitation; semi-open impeller; flow visualization; speed limitation; computational fluid dynamics; experimental verification; Pv (Pa), N (rpm).**

Abbreviations

CFD	Computational Fluid Dynamic
LE	Leading Edge
MFP	Modular Fluid Power
VDAS	Versatile Data Acquisition System
RANS	Reynolds-averaged Navier-Stokes
URANS	unsteady Reynolds-averaged Navier–Stokes
hp	Horsepower

I. INTRODUCTION

The undesirable hydrodynamic phenomenon that appears in hydraulic machinery and can develop in fluid flow is related to the circumferential speed and the parameters of the impeller geometry and causes liquid evaporation and the generation of vapor bubbles in the low-pressure region when the static pressure becomes lower than the vapor pressure of the fluid (Pv). The closest surface of the bubbles may be affected by the cavitation erosion due to the strong cavity implosions where the bubbles strike this surface as a water jet, as shown in Fig. 1. Whereas cavitation is a phenomenon related to and comes from the Latin word 'cavus', which means hollow or cavity [1].

Such vapor cavities are common in centrifugal pumps, towards the suction of the impeller at the leading edge (LE) of the blades, where the flow is accelerated as it enters the rotating impeller. These bubbles travel downstream from the impeller, where the static pressure increases, and they are reliquefied within a few milliseconds. This violent procedure generates high-intensity micro-jets that might injure the internal metal surfaces of the pump, causing rapid and extensive wear [2], [3], [4].

ISSN: 2636 - 3712 (Printed Version)
ISSN: 2636 - 3720 (Online Version)

It was stated in [6] that if P is less than Pv, evaporation occurs, and if P is greater than Pv, condensation occurs. Cavitation causes loss and degrades the device's performance, as well as a reduction in efficiency; produces an abnormally high level of noise and vibration; damages internal parts; affects structural integrity; causes erosion of blades or casing by pitting on these surfaces; causes early bearing failure; early mechanical seal failure; and causes system breakdown, resulting in significant time and financial losses. So, cavitation detection and its severity are very essential aspects in order to improve pump maintenance and reliability [7–9].

In Fig. 1, in the final step, a water jet strikes the surface.

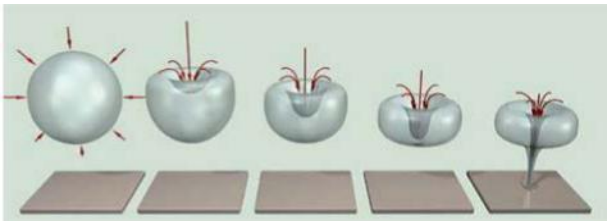

Fig. 1. Bubbles collapse due to cavitation [5]

The speed limitation [10] and [11] is a dependable strategy for controlling the harmful effects of cavitation. The formation of air bubbles can be visually observed by employing a transparent suction line and a transparent housing. When vapor bubbles move through the tube, an audible gravelling sound is created, which is also an indication of cavitation. Their findings revealed relations between speed limitation and inlet pressure, where the speed limitation was approximately proportional to the square root of the inlet pressure. Many academics are interested in the relationship between inlet pressure and rotating speed, as well as the effect on pressure and velocity variations within a pump.

Many scholars have numerically investigated cavitation in centrifugal pumps. To handle the interaction between water and vapor based on Reynolds-averaged Navier-Stokes (RANS) equations, the liquid-vapor multi-phase cavitation model was used, which considers phase change, bubble dynamics, and turbulent pressure fluctuation [12–13].

Michalis et al. [9] simulated the flow through the impeller of a centrifugal pump using the finite-volume method along with a structured grid system for the solution of the discretized governing equations. The CFD technique was applied to predict the flow patterns and pressure distribution. The proposed approach advocated a basic understanding of the flow at various operating points.

S. R. Shah et al. [15] performed a steady-state simulation of a centrifugal pump with a capacity of 200 m3/hr using RANS equations. The k-ω SST turbulence model provided better results compared to the RNG k-ε model. The characteristic curves provided by the numerical simulation were compared with the testing model's results and found to be in good agreement, providing accurate contours for the static pressure at rated discharge in the pump.

Richard et al. [16] used the multi-phase CFD method to analyze centrifugal pump performance in cavitating conditions. The two-phase RANS equations were employed, and the volume continuity and mixture momentum equations, as well as the fraction of vapor volume, were solved. Performance trends of blade cavitation and partial discharge, including breakdown, were compared to experimental measurements.

Jose Caridad et al. [17] focused on the numerical analysis of a centrifugal pump impeller of a submersible pump acting on an air-water mixture, which was similar to cavitating flow. The analysis was carried out in terms of bubble diameter and gas-void fraction. Variations in impeller head and relative flow angle at the outlet were presented as a function of liquid flow rate and phase distribution within the impeller. It was clear that the bigger the bubble diameter, the larger the head experimented with by the impeller. The numerical results and diffuser losses are in excellent agreement with the experimental results.

Krishnan et al. [18] simulated dense slurry flow through centrifugal pump casing using the Eulerian multi-phase model in FLUENT 6.1. For the discretization of momentum, a first-order upwind scheme was considered, and a mixture property-based k-ε turbulence model was used for modeling turbulence. The effects of pump flow rate, particle inlet concentration, casing width, and tongue curvature on wall stress distribution and velocities along the wall were considered. The analysis concluded that solid concentration and solid wall shear stress increased from the upstream of the tongue to the downstream of the belly region.

Inanc et al. [19] provided a numerical simulation of turbulent flows with sheet cavitation.

Fernández J. et al. [20] developed a 3-D simulation using a sliding mesh technique that accounted for the effect of blade-tongue interactions on local flow. The comparison of numerical and experimental data was acceptable, with a maximum relative error of 9% for the total head.

Barrio R. et al. [21] used Fluent to perform an internal flow analysis of a centrifugal pump and turbine modes. The simulations were carried out by solving the full unsteady Reynolds-averaged Navier-Stokes (URANS) equations by using the finite volume method with flow rates ranging from 20% and more. The numerical results were compared to the experimental measurements, which showed typical differences in the range of 3 to 5%. Internal recirculation in the runner was found in turbine mode at low and high flow rates.

Sujoy Chakraborty et al. [22] conducted a centrifugal pump numerical investigation to determine the effect of blade number and impeller speed on pump performance. Pumps with different impeller blade numbers from 4 to 12 at different speeds (2900,

3300, and 3700 rpm) were simulated using the CFD code of the commercial software ANSYS FLUENT 6.3, only to find that the pump head increased with the increase in both blade number and pump speed.

K. M. Pandey et al. [23] investigated the effect of blade number variation on pump performance while maintaining the impeller diameter and speed constant for all models. The flow through impellers with six, eight, and nine blades at a speed of 2500 rpm was studied using the standard k-e turbulence model to solve the RANS equations in ANSYS FLUENT software. Both the pump head and static pressure increased as the number of blades increased, but the efficiency variance was complicated by specific optimum values for each model.

Jintao Liu et al. [24] used a model to investigate cavitation phenomena in a pump turbine and confirmed that bubble formation near the pump's inlet could heavily reduce the machine's performance.

Sandor Bernad et al. [25] demonstrated a simulation of cavitating flows in Fluent 6.2 commercial code using the mixture model.

In the present study, the commercial CFD FLUENT 16.1 software is used. The numerical results are validated against corresponding laboratory measurements for the specific pump type used, while the exact inlet and outlet pipes, as well as other dimensions of the test rig, are simulated under the same operating conditions.

Research Steps

- Experimental work on a [0.5 hp, 1.01 L/sec, 6 m] centrifugal pump (the first pump) with a semi-open impeller and transparent housing.
- Speed limitation as a cavitation reduction solution by reducing running speed by two stages of speed reduction.
- Simulation by ANSYS-FLUENT 16.1 for the three cases of different running speeds.
- Experimental work on a [2 hp, 3.73 L/sec, 27 m] centrifugal pump (the second pump) with a semi-open impeller in another pumping system and comparing the results to the previous pump with the same percentages of speed reduction.

II. Experimental Work

For the cavitation experiments, two semi-open impeller centrifugal pumps are employed. For the cavitation studies, the first pump is a [0.5 hp, 1.01 L/sec, 6 m] pump with three blades (attached to test rig # 1), and the second pump is a [2 hp, 3.73 L/sec, 27 m] pump with six blades (attached to test rig # 2). The experimental system adopted closed-loop experimental equipment.

A. Experimental Test Rig # 1

As shown in Fig. 2, at the suction line connection, water enters the center of the impeller and flows radially through the pump. The main components of test rig #1 are shown in Table 1.

Table 1. Main components of test rig #1

Part symbol	Part Name
V1	Suction line valve
V2	Pressure line valve
V4	Drain valve
P1	0.5 hp centrifugal pump
Fl01	Flow meter [KOBOLD – DRG (10 ~ 140L/min)]
PI01	Suction line pressure gauge [GUNT-EN837-1 (-1 ~ 0 bar)]
PI02	Discharge line pressure gauge [EN837-1 (0 ~ 1.6 bar)]
SI01	Speed meter

Cavitation is easily visible by adjusting the stroboscope flash rate until the impeller appears to "freeze" due to the entire section of transparent PVC pipes and pump housing. The test pump's parameters, which include two steps of speed reduction via frequency converter (full speed is 3400 rpm, a 6% reduction in speed at 3200 rpm, and a 12% reduction in speed at 3000 rpm), are as follows:

1. At a rotational speed of 3400 rpm, the flow rate is 1.01 L/sec, and the head is 6 m.
2. At 3200 rpm, the flow rate is 0.95 L/sec, and the head is 5.5 m.
3. At 3000 rpm, the flow rate is 0.89 L/sec, and the head is 5 m.

The impeller is a semi-open type with three blades, and the inner diameter of the suction and discharge pipes is 17 mm. The flow loop system is re-circulatory. The tank is made of stainless steel, and its dimensions are 23 x 28 x 30 cm.

Fig. 2 shows the process schematic of the pump demonstrator, including all measuring points and essential components.

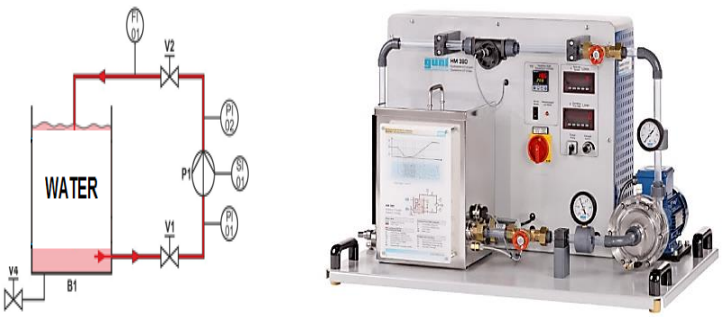

Fig. 2. Schematic diagram of the experimental test rig # 1

Performance Curve of the Test Rig # 1 Pump

The performance curve can be drawn with the suction valve fully open and the discharge valve throttled, as shown in Fig. 3.

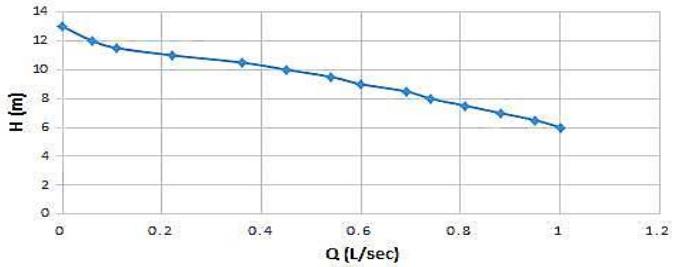

Fig. 3. Test rig # 1: first, pump performance curve at full speed; N = 3400 rpm

Cavitation as a Function of Suction Pressure: An Experimental Procedure

- Adjusting pump speed using a frequency converter
- Valves V1 and V2 are both open.
- Using valve V1, steadily throttle the suction pressure for the demonstration (at constant pump speed) and take note of the pressure and flow, as well as an increase in pump noise.
- Recording all readings for the three speeds, which are shown in Table 2.

Table 2. Measured values (for the three speeds at the start of bubbles formation)

N (rpm)	**3400**	**3200**	**3000**
Q (L/sec)	0.63	0.61	0.56
P_2 (bar)	0.26	0.24	0.21
P_1 (bar)	-0.76	-0.7	-0.6
Percentage increase in p_1 (%)	----	8%	21%
Percentage decreasing in Q (%)	----	3.5%	10.5%

In the demonstration experiment, valve V1 is used to reduce the pressure. Here we can see that the suction pressure drops further and further the more the valve is throttled; this is a clear sign that cavitation occurs as a function of pressure.

The sign of cavitation beginning can be seen at the impeller's inlet as well as after the throttle valve.

The variations in suction pressure levels can be attributable to the various throttle settings, that is, to the values that are plotted in Fig. 4.

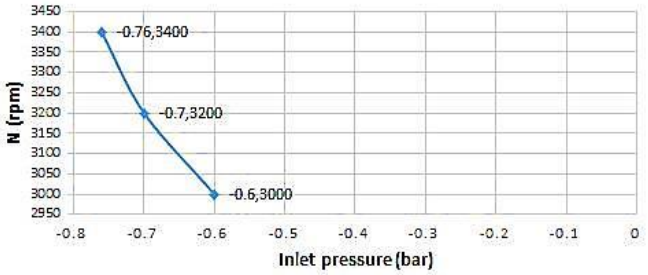

Fig. 4. Speed (rpm) Vs. inlet pressure (bar) at the start of bubbles formation for the first pump (P1)

Gas bubbles that continue on their path along the pump can be clearly visualized through the transparent casing, PVC clear pipe, and PVC connecting components.

When the flow is completely throttled, the center of the centrifugal pump clearly exhibits a gas bubble that has accumulated there. Also, the suction tube has been entirely filled with gas. Due to the centrifugal force, the remaining water is thrown outward.

The inlet pressure is presented as gauge pressure because it will be compared with the results from the numerical simulation by ANSYS software, which produce results in gauge pressure.

The air bubbles in the flow field are presented in Fig. 5 (at the same suction valve opening percentage and similar contraction). Vapor is created in the pump entry and then moves and collapses in the path of the outlet, where the pressure is rising.

The lowest amount of air bubbles inside the transparent housing is in the case of the second step of speed reduction at 3000 rpm. To further clarify the difference between the two images, black arrows have been added to the places where air bubbles collect as an indication of what happens inside the pump when the speed is reduced to reduce the harmful effect of cavitation.

Visualization setup items, including the first pump with transparent housing and the use of the stroboscope flashlight related to the running speed, are shown in Fig. 6.

A stroboscope (FLUKE® 820-2) is used to visualize flow in the 0.5 hp pump mentioned, and images are shot with a Canon® (EOS Rebel T7-SLR) digital camera as well as images of air bubbles inside the transparent casing as seen via the semi-open impeller.

To capture comparable photographs for all analyzed cases, the camera is placed towards the impeller.

At 3200 rpm

At 3000 rpm

Fig. 5. Visualization photos for the two reduction percentages of the speed

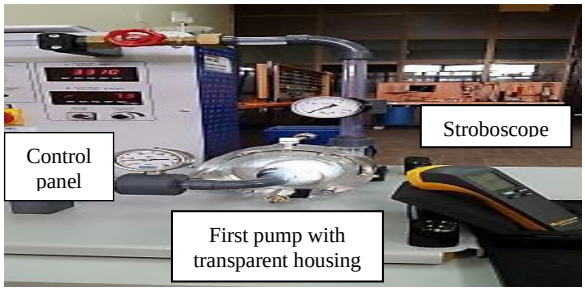

Fig. 6. Visualization setup items

B. Experimental Test Rig # 2

The centrifugal pump (which is attached to and operates an optional water turbine) is a Modular Fluid Power (MFP) test rig, complete with its pipework and a water reservoir, as well as a universal dynamometer, which measures speed, torque, and power. The dynamometer and centrifugal pump instruments are linked to VDAS (Versatile Data Acquisition System), which displays, stores, and draws charts of all-important readings.

The system is depicted in Fig. 7. Water flows from the reservoir through a strainer (filter) and one-way valve up to a pump inlet valve, then through the pump, which pushes water through an outlet valve, and then through a venturi for the flow rate measurements. And if we fit the optional turbine, then water flows from the venturi through the turbine and back down to the reservoir.

The test pump's parameters, which include two steps of speed reduction via a frequency converter, are as follows:

1. At a rotational speed of 2900 rpm, the flow rate is 3.73 L/sec, and the head is 27 m.
2. At 2725 rpm (a 6% speed reduction), the flow rate is 3.56 L/sec, and the head is 24.4 m.
3. At 2550 rpm (a 12% speed reduction), the flow rate is 3.28 L/sec, and the head is 23.3 m.

The purpose of using two test rigs is to compare two different pumps in two different pumping systems with the same reduction percentages of speed and study the effect of these

reduction percentages on the decrease in cavitation occurrence.

The impeller is a semi-open type with six blades, and the inner diameter of the suction and discharge pipes is 33 mm. The flow loop system is re-circulatory. The tank is made of plastic, and its dimensions are 55 x 105 x 50 cm.

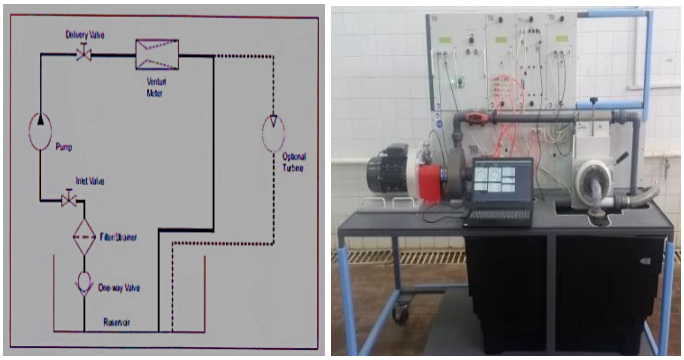

Fig. 7. Schematic diagram of the test rig # 2

- *Performance Curve of the Test Rig # 2 Pump*

The performance curve can be drawn with the suction valve fully open and the discharge valve throttled, as shown in Fig. 8.

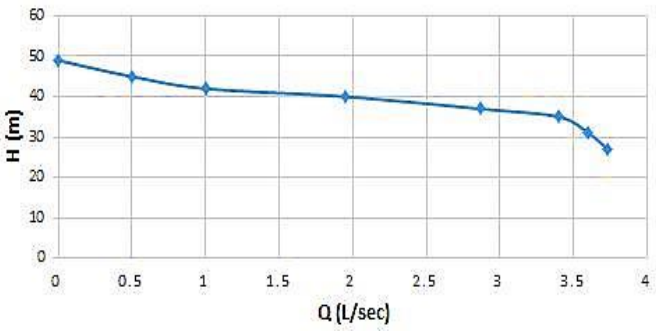

Fig. 8. Test rig #2; second pump performance curve at full speed N = 2900 rpm

- *Experimental Procedure*

  - Fully open the inlet and delivery valves.
  - Start the pump and gradually increase the speed to 2900, 2725 (a 6% reduction), and 2550 (a 12% reduction) rpm. [The percentages of speed reductions are the same as in test rig #1]. Readings for the three speeds are shown in Table 3.
  - Measure the values. Data are automatically recorded through VDAS software and an interface module.
  - Slowly close the inlet valve to decrease the inlet pressure (notice an increase in pump noise) until the flow stops (the valve is closed).

The variations in suction pressure levels can be attributable to the various throttle settings, that is, to the values that are plotted in Fig. 9.

C. Comparison Curve

As P1 percent increases, there is a convergence of results between the first and second pumps, as shown in Fig. 10. It is difficult to mention that, as a general trend, reducing the speed by certain percentages may lead to an increase in the suction pressure in equal proportions for pumps of different capacities. However, to confirm this, it is necessary to carry out more experiments for the number of pumps (more than two) of different capacities, which is not available in this research due to a lack of capabilities.

Table 3. Measured values with partial closing of the suction valve (results for the three speeds)

N (rpm)	**2900**	**2725**	**2550**
Q (L/sec)	3.53	3.34	3.11
P_2 (bar)	2.4	2.1	1.9
P_1 (bar)	-0.69	-0.64	-0.56
Percentage increase in P_1 (%)	-----	7.5%	19%
Percentage decreasing in Q (%)	-----	5.5%	12%

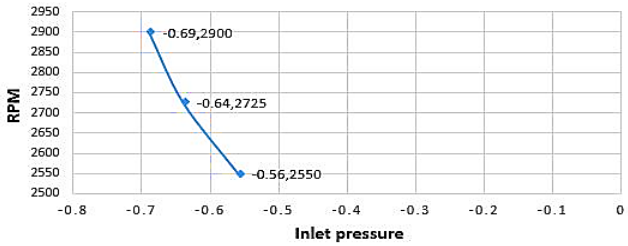

Fig. 9. Speed (rpm) vs. inlet pressure (bar) for the second pump

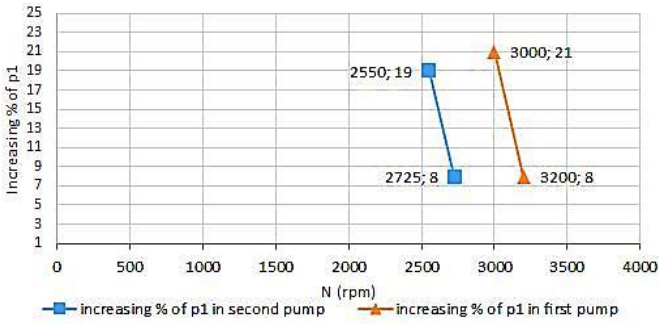

Fig. 10. Increasing percentages of p_1 for the first and second pumps

III. SIMULATION METHODOLOGY BY ANSYS-FLUENT

One of the goals of this research is to use computational approaches to understand the effects of cavitation at different rotational speeds of a centrifugal pump. The cavitation model is employed in the computational fluid dynamics (CFD) prediction, and the CFD code is used to simulate the two-phase flow (water-liquid and water-vapor). With the changes in rotational speed, the effect of cavitation on the impeller blade and inside the casing is described. Steps in numerical methodology are shown in Fig. 11.

For the performance of the centrifugal pump in this work, 3-D Reynolds-Averaged Navier-Stokes (RANS) equations are solved using CFD code to investigate the turbulent flow within the pump. The rotor (impeller) and stator (casing) are altered for transient simulation based on the angular position of the impeller [4].

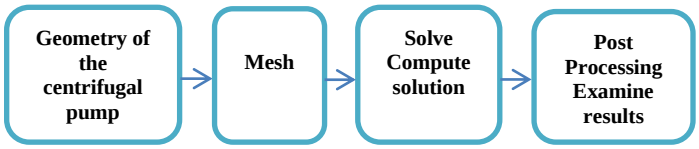

Fig. 11. Numerical methodology for the 0.5 hp centrifugal pump using CFD code

A. Geometry Drawing

The first pump's geometry (Fig. 12) is drawn using the SolidWorks 16 software.

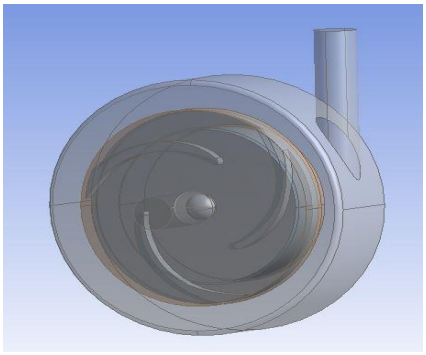

Fig. 12. First pump geometry

B. Numerical Grid and Computational Details

The flow domain is required to be discretized to convert the partial differential equations into a series of algebraic equations. This is known as grid generation.

The mesh quality directly determines the accuracy and reliability of the numerical simulation results. Structured grids are employed in this work for three computational domains: the casing inlet zone (Fig. 13), the casing zone (Fig. 14), the impeller zone (Fig. 15), and all computational domains shown in Fig. 16.

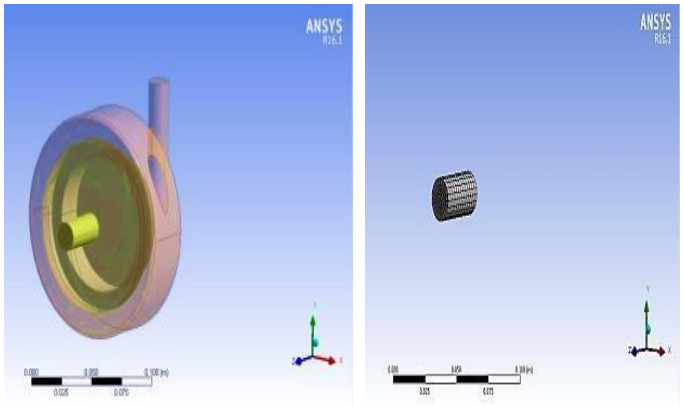

Fig. 13. Casing inlet geometry and inlet zone

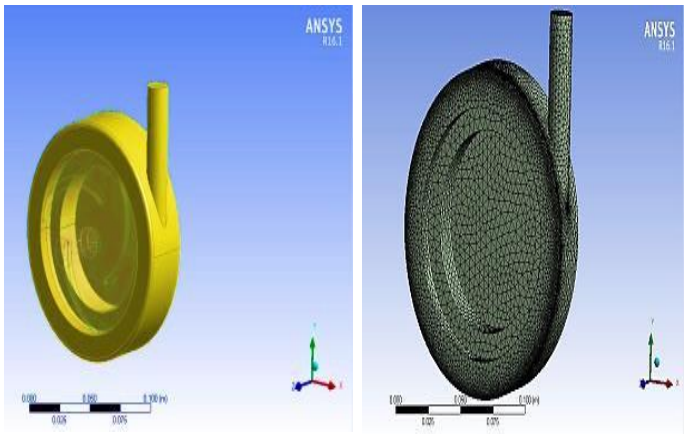

Fig. 14. Casing geometry and casing zone

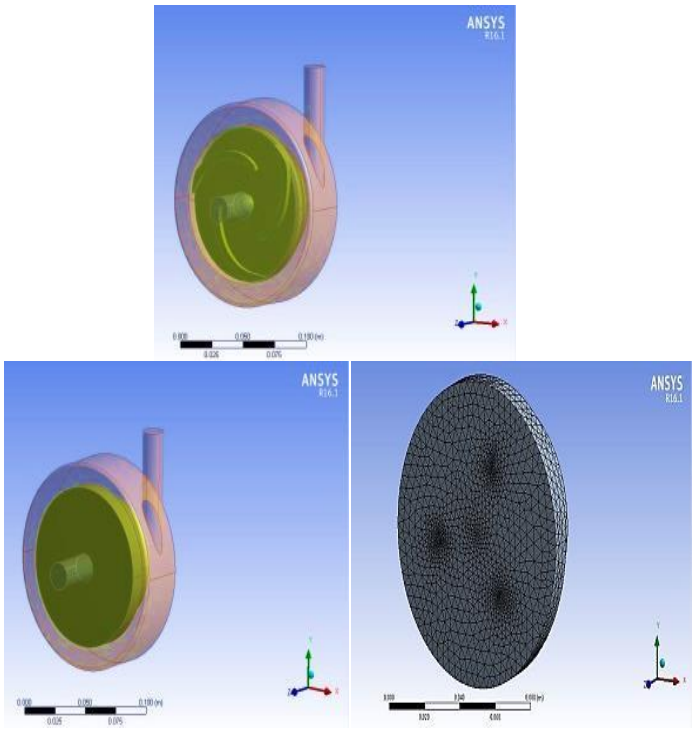

Fig. 15. Impeller and impeller zone around impeller

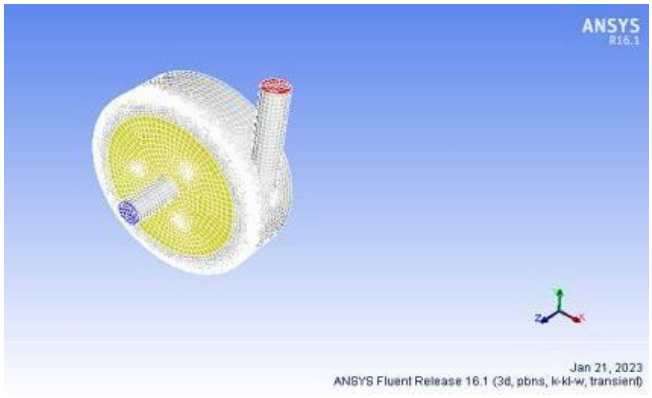

Fig. 16. All computational domains (zones)

C. Mesh Independence

In this study, a mesh independence test is done to ensure that the final mesh produces a mesh-independent solution. The grid convergence study is performed by developing four different meshes with different numbers of elements for the geometry of the pump. The number of elements for four meshes and error percentages when compared to experimental results at 3000 rpm (the best case) are summarized in Table 4, and the third mesh statistics are mentioned in Table 5.

Table 4. Elements' numbers and error percentages for each mesh

Mesh no.	**1**	**2**	**3**	**4**
No. of nodes	68427	96458	169228	252834
No. of elements	86792	122345	214644	320688
Calculated P_1 (bar)	-0.47	-0.51	-0.55	-0.564
Error %	22	15	8.5	6

Table 5. Statistics (mesh sensitivity analysis)

Total Nodes	169228
Total Elements	214644
Mesh metric	skewness
Average skewness	0.47
Approx. computational time	7 Hrs.

The smallest value of error percentage is obtained when using mesh 4, but it takes a long time to calculate (more than 16 hours), and convergence faults happen many times and interrupt it, which overloads the computer, so mesh 3 is chosen with an error percentage of 8.5% when compared to the experimental results.

On an Intel® Core TM i7-4600U CPU @ 2.7 GHz processor with 8 GB of RAM, a single run of the simulation by ANSYS 16.1 takes about 7 hours to complete the calculation process using mesh 3.

Under cavitation conditions, the impeller domain rotates on a z-axis at three speeds with varying flow operating conditions while the casing is stationary. All boundary walls are assumed to be smooth with non-slip conditions, and two contact regions are shown in Figs. 17 and 18.

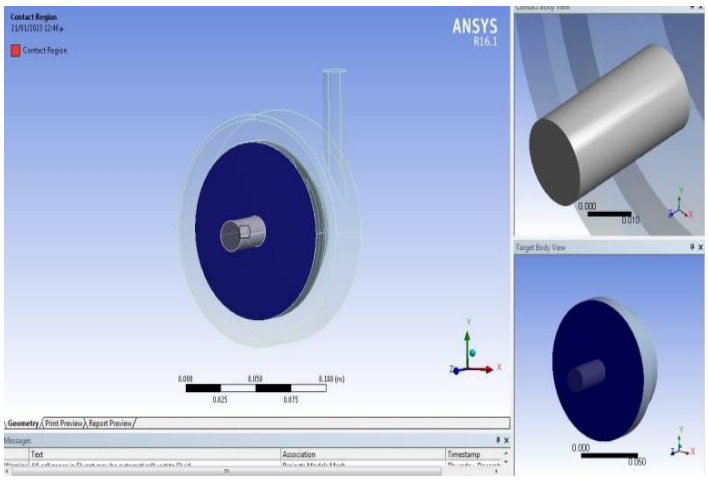

Fig. 17. Contact region 1: between casing inlet and impeller zone

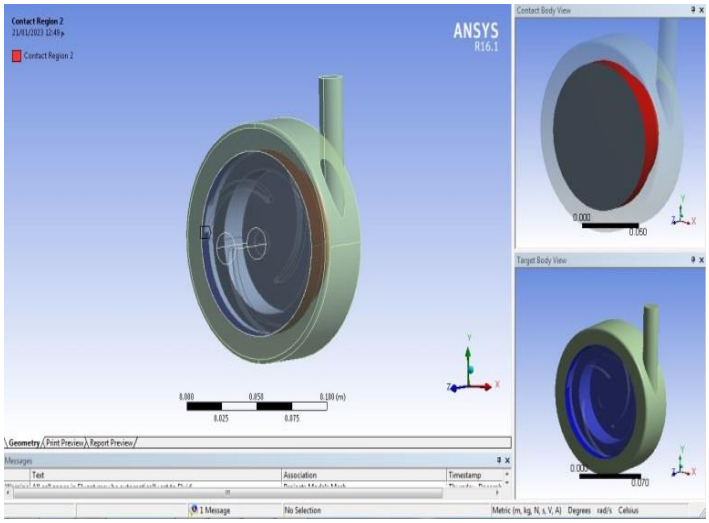

Fig. 18. Contact region 2: between impeller zone and casing

D. Boundary Conditions

The outlet boundary condition is determined using a fixed pressure gauge, and the inlet flow condition is obtained using a rotary flow meter. The readings shown in Table 6 and the inlet pressure will be obtained from ANSYS results as an indication of cavitation occurrence.

Now, the static suction pressure needs to be computed by the simulation program's solver.

Phase change, bubble dynamics, and turbulent pressure fluctuations are all described by the cavitation model [8]. The internal flow field information is obtained by solving the incompressible fluid's continuity equation and momentum equation [26].

The rotor (impeller) and stator (casing) are altered for transient simulation based on the angular position of the impeller.

Table 6. Boundary conditions

N (rpm)	3400	3200	3000
P_2 (bar)	0.26	0.24	0.21
v (m/sec)	0.31	0.3	0.28

As a result, the transition k-kl omega was designed to produce highly accurate predictions of the flow cavitation phenomenon.

All the numerically obtained results show the solutions of the iterative numerical procedure. The second order of spatial discretization is selected for pressure and momentum, and the first order is for turbulence.

A summary of the solver setting (compute solution) is shown in Table 7.

Table 7. Solver setting summary

Settings	Details	
Solver general information	Pressure based, transient	
Multiphase model	Mixture model	
	Phases	Water liquid, primary phase water vapor, secondary phase
Turbulence model	Transition k-kl omega	
Rotational zone	Impeller zone	
Pressure-Velocity coupling	Simple	
Spatial discretization	Momentum	Second order upwind
	Pressure	Second order
	Turbulent kinetic energy	First order upwind
Transient formulation	First order implicit	
Under relaxation factors	Pressure	0.3
	Momentum	0.7
	Turbulent kinetic energy	0.8
Residuals	10^{-5} Absolute	
Time step	0.0003 (No divergence fault happens during calculation until the solution is completed through the time step mentioned)	
Max Iteration / time step	1000	

E. Simulation Results and Discussion

- *Pressure Variations in the Centrifugal Pump Under Various Flow Rates*

In order to investigate the velocity and pressure variations inside a pump's flow field, numerical simulations using CFD are carried out at various flow rates.

For accurate comparison purposes, all of the static pressure contours given in the discussion and results parts are drawn on the same scale.

It is interesting to observe the pressure variations in the impeller and casing as they pass through the contour area.

Along the radial direction of the impeller, pressure gradually increases from the inlet area to the outlet area. As expected from computational results, cavitation appears at the suction region close to the leading edge (LE) of the blades.

- *The Effect of the Pump Rotational Speed on the Pressure Variations*

The effects of the pump's rotational impeller speeds are investigated, and the flow field analyses of the static pressure and velocity variations in the pump are presented in this section.

The pressure contours reflect the variations in static pressure corresponding to operating conditions.

For a precise comparison, the pressure variation contours under the various pump rotating speeds are presented on the same scale.

Fig. 19 shows that the pressure gradually increases from the inlet of the impeller to the outlet (through the inlet, outlet, and pressure contour plan) and reaches its maximum value at the outlet of the impeller blades, with the lower pressure region being at the impeller's eye.

This flow behavior within a pump was noticed in all of the above cases under investigation. In addition, it is obvious that the pressure values increase as the rotational impeller speed increases, with the highest pressure achieved at N = 3400 rpm.

Based on the above results, it is clear that the pump's rotational speed has a high effect on pressure variations.

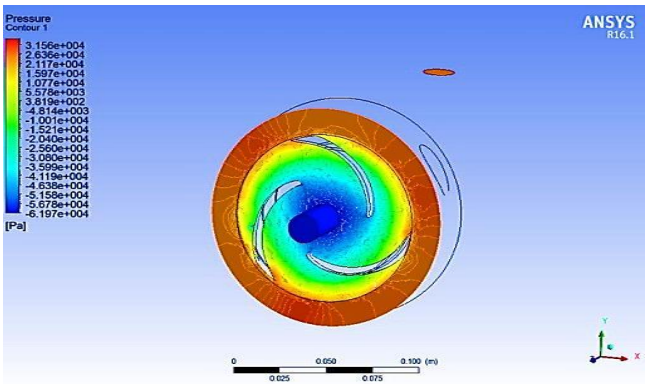

At 3400 rpm

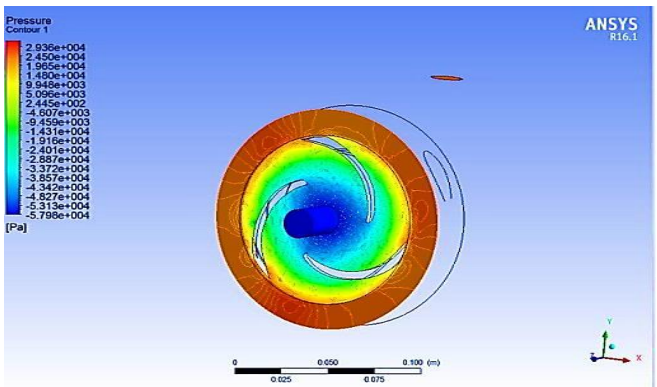

At 3200 rpm

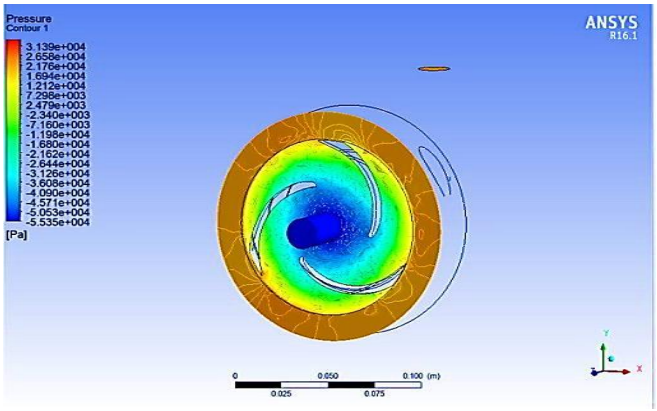

At 3000 rpm

Fig. 19. Pressure contours for the three speeds

- *Velocity Variations in Centrifugal Pump Under Various Flow Rates*

For accurate comparison purposes, all of the velocity magnitude contours at various flow rates displayed in the discussion and results parts are drawn on the same scale.

An interesting point to note is that there are various flow velocities across the impeller blades and inside the casing.

Also, by decreasing rotational speed, circulation, vortex, and rabid mixing are decreased (from streamlines, which are shown in Fig. 20).

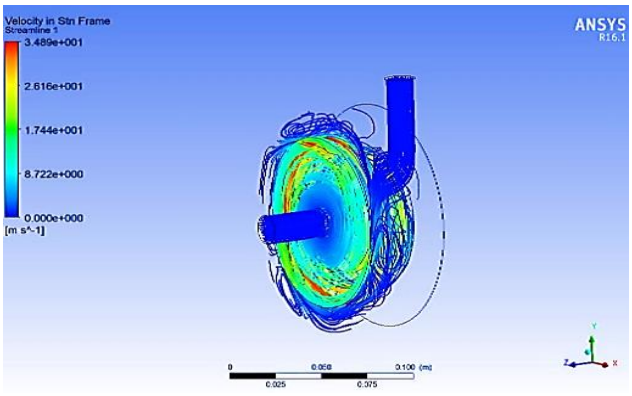

At 3400 rpm

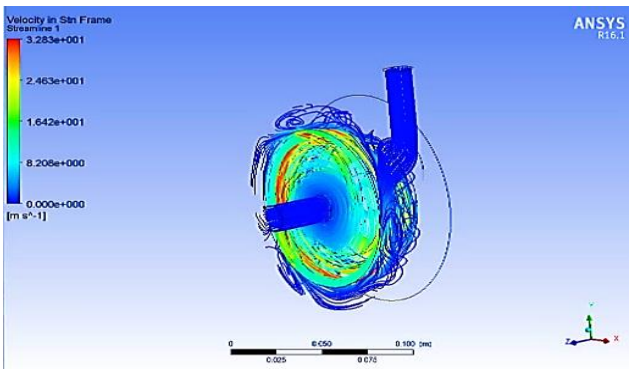

At 3200 rpm

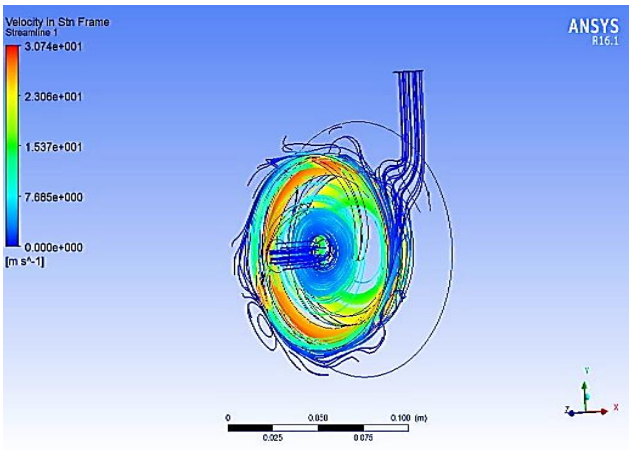

At 3000 rpm

Fig. 20. Streamlines for the three speeds

- *The Effect of Pump Rotational Speed on Velocity Variations*

The effects of the rotational impeller speeds of the pump are investigated. The flow field analyses of the velocity variations in the pump are presented on a similar scale in the velocity vectors under the different pump rotational speeds (3000, 3200, and N = 3400 rpm).

It can be observed that for different pump rotational speeds, the velocity magnitude inside a pump is gradually increased from the impeller's inlet to the outlet.

In all cases under investigation, the velocity magnitude in the impeller is greater than that in the casing. Furthermore, it is obvious that the magnitude of the velocity increases as the rotational speed of the pump increases, and a higher velocity is observed at N = 3400 rpm.

In Fig. 21, the velocity shows that the pump's rotational speed has a high effect on the velocity of the centrifugal pump.

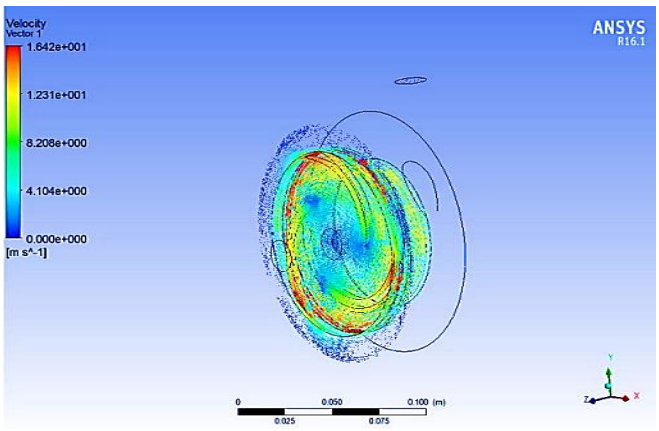

At 3400 rpm

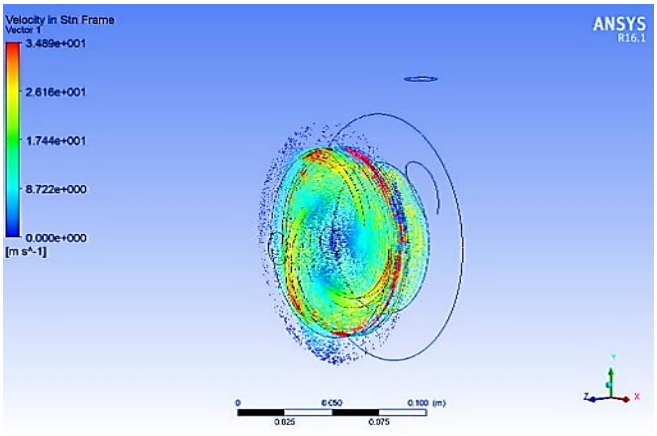

At 3200 rpm

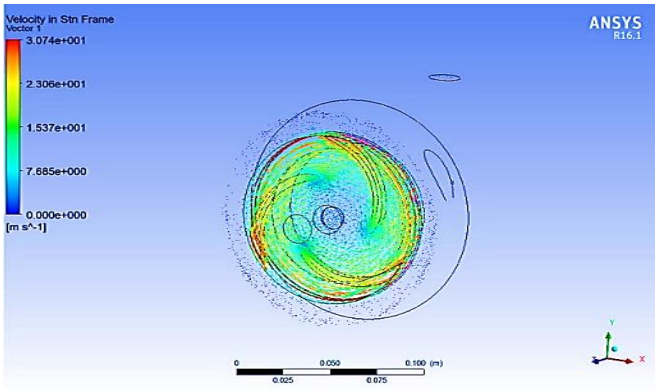

At 3000 rpm

Fig. 21. Velocity vectors of the three speeds

It may be noted from Fig. 21 that, in the second step of speed reduction (at 3000 rpm), velocity at suction is reduced when compared with the other speeds, which will decrease cavitation occurrence at suction.

IV. Comparison of the CFD Model and Experimental Results

When performing numerical investigations, one of the most significant steps is the validation of the outcomes. In other words, the numerical simulation results are compared with experimental data to verify accurately that the numerical model represents the physical model of the actual system. As a result, in validation investigations, the entire set of geometric, flow, and solver-related parameters and variables becomes vital [4].

The computed static suction pressure for cavitating flow is the result that we need to obtain from simulation and compare to the experimental results.

The accuracy of the numerical simulation method in this work is verified by comparing experimental data with numerical results, as shown in Fig. 22.

The numerical method is verified to guarantee the accuracy and dependability of the results and the internal flow field [10].

In the best case, there is an acceptable agreement between the numerical and experimental results, with an error percentage of 8.5% for the suction pressure value as shown in Table 8.

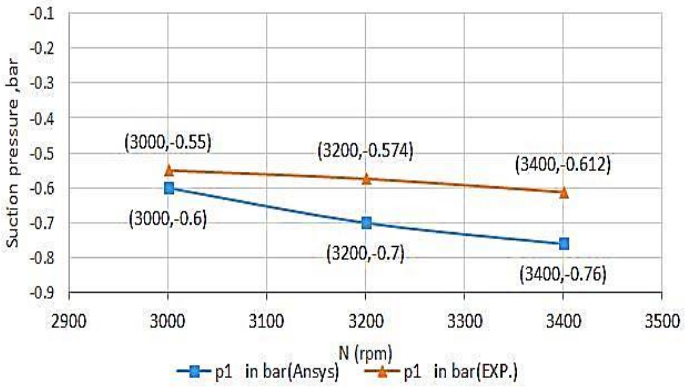

Fig. 22. Suction pressure (bar) in ANSYS and experimental results in the first pump

Table 8. Results from ANSYS and error percentages

N (rpm)	3400	3200	3000
Suction pressure(bar)	-0.612	-0.574	-0.55
Error %	19%	18%	8.5%

The relation between suction pressure and flow rate in the first pump at the three speeds is related to readings, which are mentioned in Table 2, and boundary conditions, which are mentioned in Table 6 and plotted in Fig. 23.

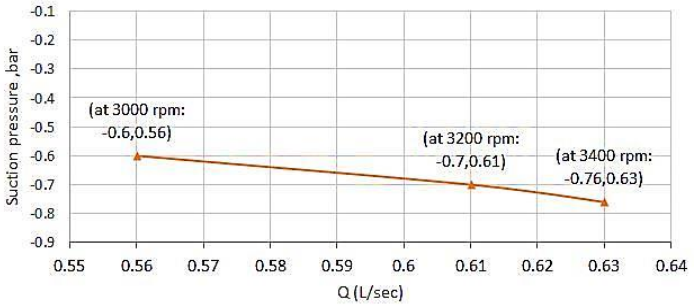

Fig. 23. Suction pressure (bar) vs. flow rate (L/sec) in the first pump

- *Validation of numerical and experimental results*

The difference between numerical and experimental results might be caused by several reasons. First, there are mechanical losses in the pump, which are caused by contact between the shaft and the bearings and between the shaft and the seal. The second reason is the gap between the casing and impeller. Third, hydraulic losses are caused by friction losses, vortexes, and separation due to flow direction change that

happens at the passages of the impeller. In addition, the pump's geometry and flow field are complicated and turbulent, with impeller blade curvature having a significant effect on the flow field developed either within the blade passages or inside the casing.

V. Conclusion

The cavitation phenomenon is globally understood as the formation of vapor bubbles in a fluid flow due to a pressure drop below its vapor pressure. Cavitation detection requires advanced methods because of its rapid and complicated nature; otherwise, it can only be detected by its effects on the equipment, such as unusual noise, vibrations, and material damage, based on the physical and operational conditions of the system in fluid machinery [27].

A comprehensive investigation was carried out to monitor cavitation within a centrifugal pump under a wide range of operating conditions. The following conclusions are obtained from this study's analysis, results, and discussion:

A. Experimental Work

This study investigates the cavitation phenomenon in a centrifugal pump with a semi-open impeller that has three blades. In order to study the cavitation behavior, the machine's casing is made from Plexiglas in order to visualize the flow through the passage where cavitation dominates the flow and creates a very turbulent and noisy environment, which is depicted in photos taken from the impeller.

1. The level of cavitation within a centrifugal pump has been directly related to the pump flow rate and pump rotational speed; when full speed is 3400 rpm, speed reduction percentages are 6% at 3200 rpm and 12% at 3000 rpm, with increasing percentages in suction pressure of 8% and 21%, respectively.
2. Under the cavitation process, the vapor bubbles are formed due to a decrease in fluid pressure, which is lower than the vapor pressure. Moreover, they have a significant effect on the flow within a pump.
3. The inception of the cavitation process mostly occurred near the impeller's eye, around or close to the impeller blades' leading edges.
4. Percentage increase of suction pressure; P_1 for the second pump (6% speed reduction at 2725 rpm) to decrease the harmful effect of cavitation = 7.5%.
5. Percentage increase of suction pressure; P_1 for the second pump (12% speed reduction at 2550 rpm) to decrease the harmful effect of cavitation = 19%.

B. Numerical Simulation

The results also reveal that cavitation can be detected experimentally and numerically.

Flow analysis of centrifugal pumps is often a challenging task because it requires the study of highly complicated flow that is turbulent, three-dimensional, and has a rapidly changing curvature of the flow passage.

The CFD approach has been widely used in centrifugal pumps as a numerical simulation tool for performance prediction, analysis of interaction effects in different components to obtain a reasonable estimation of the centrifugal pump's overall performance, and comparing the results with experimental data with typical errors of acceptable percentages.

An experimental test rig was designed to test a centrifugal pump (with a radial semi-open impeller) under cavitating conditions at various speeds and flow rates, and it is compared to an ANSYS 16.1 (FLUENT solver) multiphase 3D model. In order to study the pump's performance, the computational domain includes the suction tube, impeller, and casing. The analysis revealed good consistency, as the CFD model trends are in acceptable agreement with the experiments, with an error percentage of 8.5% for the best case.

The static pressure distributions through the impeller and casing are predicted by the cavitation model. Also, in the low-pressure area near the blade suction side at the inlet, pressure contours can be obtained, as can velocity distributions obtained from velocity vectors and streamline plots.

- *Statement on Equipment and Test Benches*

This study was completed (with equipment and test benches) in the Hydraulics Training Center of the Hydropower Station Generation company in Egypt.

- *Declarations*

Statement of the Author's Contribution Mina Luke Kerellous: [through five years] conducted the experiments, analyzed and interpreted the data, carried out a simulation of pump operation by ANSYS-FLUENT, and wrote the first draft of this paper.

References

[1] Georgios Mousmoulis, Ioannis Kassanos, George Aggidis, and Ioannis Anagnostopoulos, "Numerical simulation of the performance of a centrifugal pump with a semi-open impeller under normal and cavitating conditions", Applied Mathematical Modelling, Vol. 89, Part 2, pp. 1814-1834, 2021, ISSN 0307-904X.

[2] G. Mousmoulis, N. Karlsen-Davies, G. Aggidis, J. Anagnostopoulos, and D. Papantonis, "Experimental analysis of the onset and development of cavitation in a centrifugal pump", Journal of Physics: Conference Series, Series 813 012044, 2017.

[3] Rakibuzzaman, No-Hyun Park, Sang-Ho Suh, "Analysis of Cavitation with Rotational Speed and Water Temperature Changes of Centrifugal Pump", Journal of the Korean Society of Fluid Mechanics, Vol. 20, No. 5, October 2017, pp. 40~45, 2017, ISSN (Print): 2287-9706.

[4] Al-Obaidi A. R., "Experimental and numerical investigations on the cavitation phenomenon in a centrifugal pump", doctoral thesis, University of Huddersfield, 2018.

[5] Al-Obaidi A. R., "Experimental investigation of the effect of suction valve opening on the performance and detection of cavitation in the centrifugal pump based on acoustic analysis technique", Archives of Acoustics, Vol. 44, No. 1, pp. 59~69, 2019.

[6] Md Rakibuzzaman, Kyungwuk Kim, and Sang-Ho Suh, "Numerical analysis of cavitation phenomena with variable-speed centrifugal pump", Journal of Power Technologies, Vol. 96, No. 4, pp. 306~311, 2016.

[7] P. J. McNulty, and I. S. Pearsall, "Cavitation inception in pumps", Journal of Fluids Engineering, Vol. 104, pp. 99~104, 1982.

[8] Al-Obaidi A.R., Mishra R., "Experimental investigation of the effect of air injection on performance and detection of cavitation in the centrifugal pump based on vibration technique", Arabian Journal for Science and Engineering, Vol. 45, pp. 5657~5671, 2020.

[9] Michalis D. Mentzos, Andronicos E. Filios A. E., Dionisios P. Margaris, and Dimitrios G. Papanikas, "CFD predictions of flow through a centrifugal pump impeller", 1st International Conference on Experiments, Processes, System Modeling, Simulation, and Optimization, Athens, 6-9 July 2005.

[10] Qun Chao, Jianfeng Tao, Junbo Lei, Xiaoliang Wei, Chengliang Liu, Yuanhang Wang, and Linghui Meng, "Fast scaling approach based on cavitation conditions to estimate the speed limitation for axial piston pump design", Frontiers of Mechanical Engineering, Vol. 16, pp. 176-185, 2021.

[11] Krishnachandran, A. Samson, and Akash Rajan, "Condition monitoring of cavitation-induced centrifugal pump", Recent Asian Research on Thermal and Fluid Sciences, Springer, Singapore, pp. 393-408, 2020.

[12] Aldo Iannetti, Matthew T. Stickland, and William M. Dempster, "A CFD and experimental study on cavitation in positive displacement pumps: Benefits and drawbacks of the full cavitation model", Engineering Applications of Computational Fluid Mechanics, Vol. 10.1, pp. 57-71, 2016.

[13] Xue-lin Tang, Li-yuan Bian, Fu-jun Wang, Xiao-qin Li, and Man Hao, "Numerical investigations on cavitating flows with thermodynamic effects in a diffuser-type centrifugal pump", Journal of Mechanical Science and Technology, Vol. 27, pp. 1655-1664, 2013.

[14] Al-Obaidi Ahmed Ramadhan, "Experimental Comparative Investigations to Evaluate Cavitation Conditions within a Centrifugal Pump Based on Vibration and Acoustic Analysis Techniques", Archives of Acoustics, Vol. 45, No. 3, pp. 541-556 ,2020.

[15] S. R. Shah, S. V. Jain, and V. J. Lakhera, "CFD-based flow analysis of centrifugal pumps", Proceedings of the 37th National and 4th International Conference on Fluid Mechanics and Fluid Power. IIT Madras, Chennai, India, 2010.

[16] Richard B. Medvitz, Robert F. Kunz, David A. Boger, Jules W. Lindau, Adam M. Yocum and Laura L. Pauley, "Performance Analysis of Cavitating Flow in Centrifugal Pumps Using Multiphase CFD", Journal of Fluids Engineering, 124(2): 377-383, 2002.

[17] Jose Caridad, Miguel Asuaje, Frank Kenyery, Andrés Tremante, and Orlando Aguillón, "Characterization of a Centrifugal Pump Impeller under Two-Phase Flow Conditions", Journal of Petroleum Science and Engineering, Vol. 63, Issues 1-4, pp. 18~22, 2008, ISSN 0920-4105.

[18] Krishnan V. Pagalthivarthi, Pankaj K. Gupta, Vipin Tyagi, and M. R. Ravi, "CFD Predictions of Dense Slurry Flow in Centrifugal Pump Casings", International Journal of Mechanical and Mechatronics Engineering, Vol. 5, No. 3, pp. 538~550, 2011.

[19] Inanc Senocak and Wei Shyy, "Numerical simulation of turbulent flows with sheet cavitation", In CAV 2001: Fourth International Symposium on Cavitation, June 20-23, 2001, California Institute of Technology, Pasadena, CA, USA.

[20] Fernández J, Barrio R, Blanco E, Parrondo JL, and Marcos A. "Numerical Investigation of a Centrifugal Pump Running in Reverse Mode", Proceedings of the Institution of Mechanical Engineers, Part A: Journal of Power and Energy, Vol. 224, Issue 3, pp. 373~381, 2010.

[21] Barrio R, Fernández J, Blanco E, Parrondo J, and Marcos A., "Performance Characteristics and Internal Flow Patterns in a Reverse-Running Pump-Turbine", Proceedings of the Institution of Mechanical Engineers, Part C: Journal of Mechanical Engineering Science, Vol. 226, Issue 3, pp. 695~708, 2012.

[22] Sujoy Chakraborty, K. M. Pandey, and Bidesh Roy, "Numerical Analysis on Effects of Blade Number Variations on Performance of Centrifugal Pumps with Various Rotational Speeds", International Journal of Current Engineering and Technology, Vol. 2, No. 1, pp. 143~152, March 2012, ISSN 2277-4106.

[23] K. M. Pandey, A. P. Singh, and Sujoy Chakraborty, "Numerical studies on effects of blade number variations on performance of centrifugal pumps at 2500 rpm", Journal of Environmental Research and Development, Vol. 6, No. 3A, pp. 863~868, 2012.

[24] Jintao Liu, Shuhong Liu, Yulin Wu, Lei Jiao, Leqin Wang, and Yuekun Sun, "Numerical investigation of the hump characteristic of a pump-turbine based on

an improved cavitation model", Computers & Fluids, Vol. 68, pp. 105-111, 2012, ISSN 0045-7930.

[25] Sandor Bernad, Romeo Susan-Resiga, Sebastian Muntean, and Ioan Anton, "Numerical analysis of the cavitating flows", Proceedings of the Romanian Academy, Series A, Vol. 7, No. 1, pp. 33-45, 2006.

[26] Wang L, Lu J, Liao W, Zhao Y, and Wang W., "Numerical simulation of the tip leakage vortex characteristics in a semi-open centrifugal pump", Applied Sciences, Vol. 9, No. 23, 5244, 2019.

[27] Maxime Binama, Alex Muhirwa, and Emmanuel Bisengimana, "Cavitation effects in centrifugal pumps: A review", International Journal of Engineering Research and Applications, Vol. 6, Issue 5, Part 1, pp. 52-63, May 2016, ISSN: 2248-9622.

[28] S. R. Shah, S. V. Jain, R. N. Patel, and V. J. Lakhera, "CFD for centrifugal pumps: a review of the state-of-the-art", Procedia Engineering, Vol. 51, pp. 715-720, 2013, ISSN 1877-7058.

[29] Mahesh M. Athavale, H. Y. Li, Yu Jiang, and Ashok K. Singhal, "Application of the full cavitation model to pumps and Inducers", International Journal of Rotating Machinery, Vol. 8(1), pp. 45-56, 2002.

[30] ANSYS Turbo-Grid Reference Guide, (www.ansys.com): The official website of ANSYS.